Alloy Formation of Gold−Silver Nanoparticles and the Dependence of the Plasmon Absorption on Their Composition

S. Link,[†] Z. L. Wang,[‡] and M. A. El-Sayed*,[†]

Laser Dynamics Laboratory, School of Chemistry and Biochemistry, and School of Materials Science and Engineering, Georgia Institute of Technology, Atlanta, Georgia 30332-0400

Gold−silver alloy nanoparticles with varying mole fractions are prepared in aqueous solution by the co-reduction of chlorauric acid $HAuCl_4$ and silver nitrate $AgNO_3$ with sodium citrate. As the optical absorption spectra of their solutions show only one plasmon absorption it is concluded that mixing of gold and silver leads to a homogeneous formation of alloy nanoparticles. The maximum of the plasmon band blue-shifts linearly with increasing silver content. This fact cannot be explained by a simple linear combination of the dielectric constants of gold and silver within the Mie theory. On the other hand, the extinction coefficient is found to decrease exponentially rather than linearly with increasing gold mole fraction x_{Au}. Furthermore, the size distribution of the alloy nanoparticles is examined using transmission electron microscopy (TEM). High-resolution TEM (HRTEM) also confirms the formation of homogeneous gold−silver alloy nanocrystals.

Introduction

The intense research in the field of nanoparticles by chemists, physicists, and materials scientists is motivated by the search for new materials in order to further miniaturize electronic devices as well as by the fundamental question of how molecular electronic properties evolve with increasing size in this intermediate region between molecular and solid-state physics.[1−7] Possible future applications include the areas of ultrafast data communication and optical data storage.[4−6] Semiconductor nanoparticles are also used in building solar cells[7] and metal nanoparticles are very important as catalysts because of their high surface-to-volume ratios.[4]

Metal nanoparticles have mainly been studied because of their unique optical properties as especially nanoparticles of the alkali metals and the noble metals copper, silver, and gold have a broad absorption band in the visible region of the electromagnetic spectrum.[8−15] Solutions of these metal nanoparticles show a very intense color, which is absent for the bulk material as well as for the atoms. Their origin is attributed to the collective oscillation of the free conduction electrons induced by an interacting electromagnetic field. These resonances are also denoted as surface plasmons.

Mie[16] was the first to explain this phenomenon by applying classical electrodynamics to spherical particles and solving Maxwell's equations for the appropriate boundary conditions. The total extinction cross section composed of absorption and scattering is given as a summation over all electric and magnetic multipole oscillations. The Mie theory has the advantage of being conceptually simple and has found wide applicability in explaining experimental results.[8,9,14,15] However, all of the material properties are represented by a complex dielectric function of the absorbing metal nanoparticles thus obscuring somehow the underlying microscopic events, such as the possible decay mechanisms of the coherent motion of the free electrons.

Gold and silver nanoparticles have been studied in great detail.[1,2,8,15,17] Especially, the size effect on the plasmon absorption in connection with the Mie theory and its modifications has been of major interest.[8,17] Alloy nanoparticles, on the other hand, have mainly been studied because of their catalytic effects.[18,19] As gold has low catalytic activity compared to platinum or palladium, the structural and catalytic changes have been examined for the admixture of platinum or palladium to gold.[20−24]

Studies on the Au−Ag system include the following. Papavassiliou[25] prepared 10 nm gold−silver alloy nanoparticles in 2-butanol by evaporation and condensation of the alloys. A linear dependence of the plasmon absorption maximum on the composition of the nanoparticles was found. Alloy clusters with diameters between 9 and 15 nm were obtained in photosensitive glasses.[8,26] The disadvantage of this preparation method is, however, the fact that an increasing silver content also results in larger particles. Liz-Marzan et al.[27] used inorganic fibers in aqueous solution for the stabilization of gold−silver particles with diameters of 2 to 3 nm after the simultaneous reduction of gold and silver salts by sodium borohydride. Teo et al.[28] synthesized a 38 atom gold−silver cluster ($Au_{18}Ag_{20}$). The solution of this cluster showed a single absorption peak at 495 nm. Mulvaney et al.[15,29] and also Sinzig et al.[8,26] prepared silver nanoparticles coated with an overlayer of gold (core−shell nanoparticles). These particles have two distinct plasmon absorption bands and their relative intensities depend on the thickness of the shell. But also alloy formation within the shell was suggested on the basis of the optical absorption spectra. Similarly, gold−silver composite colloids (30−150 nm in diameter) consisting of mixtures of gold and silver domains were obtained by irradiating aqueous solutions of gold and silver ions with 253.7 nm UV light.[30] Those nanoparticles also showed two plasmon absorption bands originating from the individual gold and silver domains.

It is shown in this letter how gold−silver alloy nanoparticles can be obtained by simple co-reduction of chlorauric acid $HAuCl_4$ and silver nitrate $AgNO_3$ with sodium citrate in aqueous

* Corresponding author.
† Laser Dynamics Laboratory, School of Chemistry and Biochemistry.
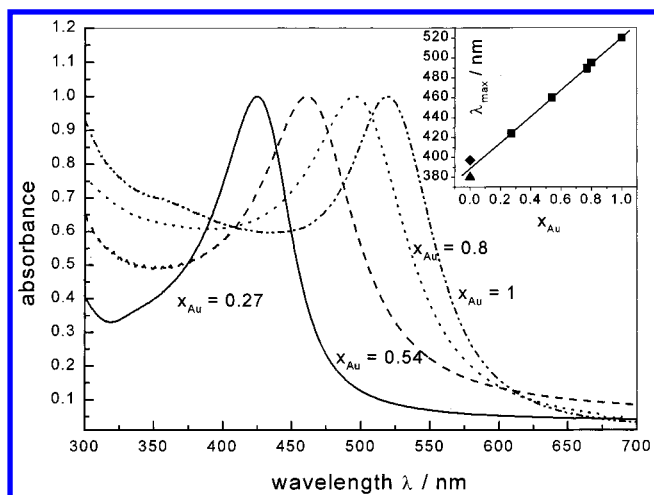‡ School of Materials Science and Engineering.

Figure 1. UV−vis absorption spectra of gold and gold−silver alloy nanoparticles with varying gold mole fractions x_{Au}. The spectra have been normalized at the plasmon absorption maximum. The inset shows how the absorption maximum of the plasmon band depends on the composition. The solid line is a linear fit of the absorption maximum to the gold mol fraction x_{Au}. The squares correspond to the experimental data while the triangle and diamond are two literature values for pure silver nanoparticles.[29,34]

Figure 2. Extinction coefficients ϵ at the plasmon maximum as a function of the alloy nanoparticle composition. The solid spheres are results of this work while the open diamonds are taken from refs 29 and 33. The error bars correspond to twice the experimental standard deviation. The data points seem to fit an exponential (solid line) dependence better than a linear one (dashed line). The left axis displays the extinction coefficient using the molar concentration of reduced atoms in solution, while the right axis shows ϵ corresponding to 20 nm nanoparticles containing roughly 250 000 atoms.

solution. The optical properties (plasmon absorption) are examined and compared to the calculated absorption spectra using the Mie theory. Structural information is obtained from TEM and HRTEM.

Experimental Section

Gold nanoparticles are prepared following a method introduced by Turkevich.[31] An amount of 95 mL of chlorauric acid (HAuCl$_4$) solution containing 5 mg of Au is refluxed and 5 mL of 1% sodium citrate solution is added to the boiling solution. The reduction of the gold ions by the citrate ions is complete after 5 min, while the solution is further boiled for 30 min and is then left to cool to room temperature. This method yields spherical particles with an average diameter of ∼20 nm. The actual value of the mean size might vary slightly from each preparation; the size distribution, however, is found to be always ∼10%.

Gold−silver alloy particles are prepared in the same way by substituting a predetermined number of moles of gold atoms by the equivalent number of moles of silver atoms in the form of silver nitrate AgNO$_3$. Mixed particles with gold mole fractions x_{Au} of 0.27, 0.54, 0.77, and 0.8 are made by this method. Silver nanoparticles in this size range, however, could not be obtained by the reduction with sodium citrate.

The size of the particles is analyzed by TEM using a Hitachi HF-2000 field emission TEM operating at 200 kV. From the TEM images the size distributions of the different samples are determined by counting at least 300 particles. The HRTEM studies are carried out with a JEOL 4000EX HRTEM operating at 400 kV. The UV−vis absorption spectra are recorded on a Beckman DU 650 spectrophotometer in a 1 cm glass cuvette.

Results

If gold and silver ions are reduced simultaneously by sodium citrate in the same solution, gold−silver alloy particles are formed. The alloy formation is concluded from the fact that the optical absorption spectrum shows only one plasmon band.[15,25,32] Two bands would be expected for the case of a mixture of gold and silver nanoparticles. Figure 1 shows the
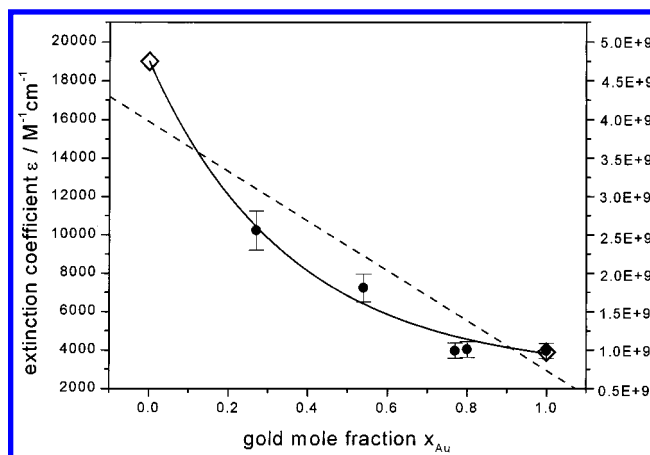
absorption spectra for gold and several gold−silver alloy nanoparticles with varying silver content. The plasmon band is blue-shifted with an increasing amount of silver. In the inset the plasmon maximum λ_{max} is plotted against the gold mole fraction x_{Au} and a linear relationship is found. The two points for the position of the plasmon absorption of silver nanoparticles are taken from the literature,[29,34] as pure silver particles of similar size could not be obtained by the same method as used for the gold and alloy particles.

The extinction coefficients ϵ at the plasmon maximum for the prepared samples are displayed in Figure 2 as a function of the gold mole fraction x_{Au}. The extinction coefficient per metal atom (left axis) is calculated with the known metal salt concentration before reduction with sodium citrate assuming that all metal ions are reduced. The extinction coefficient per nanoparticle is shown on the right axis. For comparison, a particle diameter of 20 nm consisting of roughly 250 000 atoms is assumed for all samples. Note that a value of 1×10^9 M^{-1} cm^{-1} for a molar extinction coefficient of 20 nm gold nanoparticles is about 3 orders of magnitude larger than for a typical organic molecule[35] and increases with increasing particle size as it scales with the volume of the particle (see also eq 1 below). Equivalently, this corresponds to an absorption cross section of about 166 nm^2 for 20 nm nanoparticles which is roughly 50% of their actual size. An extinction coefficient of 4000 M^{-1} cm^{-1} per atom for the gold nanoparticles is, furthermore, in close agreement with a value of 3900 M^{-1} cm^{-1} determined by Henglein et al.[33] which is included in Figure 2 (open diamomds) together with the extinction coefficient of pure silver particles measured by the same author. The solid line in Figure 2 is an exponential fit to the data points, while the dashed line is obtained from a linear fit. Even considering the error bars, which represent twice the experimental standard deviation, an exponential dependence of the extinction coefficient on the composition of the nanoparticles describes the experimental data better than a linear relationship as found for the plasmon band maximum.

Figure 3a shows a TEM image of a self-assembly of gold−silver alloy nanoparticles with a gold mole fraction of 0.8. Their average size is determined to be 18 nm. The corresponding size histogram is given in Figure 3c. The average sizes of the other
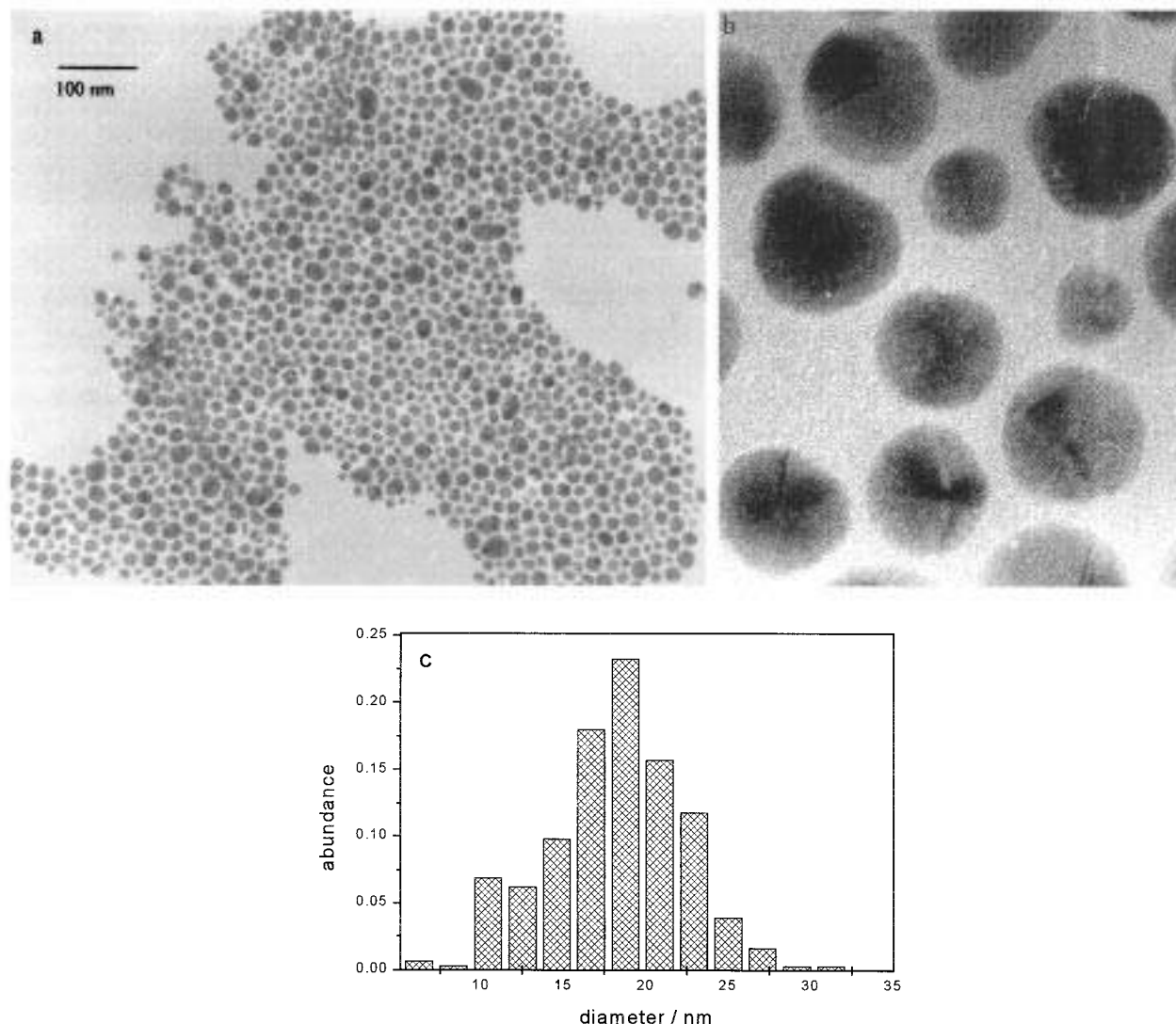
Letters

J. Phys. Chem. B, Vol. 103, No. 18, 1999 **3531**

Figure 3. (a) TEM image of gold−silver alloy nanoparticles. The gold mole fraction x_{Au} of the alloy particles is 0.8. The corresponding absorption spectrum is shown in Figure 1. (b) HRTEM image showing the individual lattice planes as well as the defect structures of the alloy nanoparticles ($x_{Au} = 0.8$). (c) Size histogram corresponding to the sample shown in (a). The mean size is determined to be 18 nm.

particles are 17 nm ($x_{Au} = 0.27$), 25 nm ($x_{Au} = 0.54$), 17 nm ($x_{Au} = 0.77$), and 22 nm (pure gold). The small variation in size results from the fact that the reduction with sodium citrate produces a homogeneous size distribution of nanoparticles but with a slightly different mean size for every preparation.[31] This difference in sizes, however, should have no or only a small effect on the plasmon band maximum.[8]

HRTEM studies on the gold−silver alloy nanoparticles with $x_{Au} = 0.8$ reveal the presence of defect structures. Most nanoparticles contain single and multiple twins as well as stacking faults[36] in agreement with the structure of pure gold particles prepared in the same way or by other methods.[37−40] Figure 3b shows a typical example of these defect structures. The individual lattice planes are clearly visible in this picture. These investigations also confirm that no lattice mismatch is introduced by the incorporation of silver atoms. This is expected as gold and silver have very similar lattice constants of 0.408 and 0.409 nm.[41,42] In fact, the difference in lattice constants is smaller than the amplitude of thermal vibrations of the atoms. This gives another indication that a complete alloy formation takes place even for nanometer size particles. Because of the very similar lattice constants of gold and silver and from the

known fact of alloy formation of these two metals in the bulk phase[43] this result is expected.

Discussion

While the structural information about the gold−silver alloy nanoparticles presented so far is not very surprising, the linear dependence of the plasmon maximum on the composition, however, deserves some further discussion. Following the Mie theory, for nanoparticles small compared to the wavelength of the exciting light ($\lambda \gg 2R$, for gold $2R < 25$ nm [8]) only the dipole absorption contributes to the extinction cross section σ_{ext} of the particles (quasi-static or dipole approximation)[8,9,12−14]:

$$\sigma_{ext} = \frac{9V \cdot \epsilon_m^{3/2}}{c} \cdot \frac{\omega \cdot \epsilon_2(\omega)}{[\epsilon_1(\omega) + 2 \cdot \epsilon_m]^2 + \epsilon_2(\omega)^2} \tag{1}$$

V is the spherical particle volume, c the speed of light, ω the angular frequency of the exciting radiation, and ϵ_m and $\epsilon(\omega) = \epsilon_1(\omega) + i\epsilon_2(\omega)$ denote the dielectric functions of the surrounding medium (assumed to be frequency independent) and of the particle material, respectively.

From eq 1 it follows that resonance occurs when $\epsilon_1(\omega) \approx -2\epsilon_m$ if ϵ_2 is small. The bandwidth and peak height are roughly determined by $\epsilon_2(\omega)$.[8,17] In the simplest case of a free electron gas the dielectric function can be written within the Drude–Sommerfeld theory as[44,45]

$$\epsilon(\omega) = 1 - \frac{\omega_p^2}{\omega^2 + i\gamma_0\omega} \qquad (2)$$

The plasmon frequency $\omega_p^2 = (ne^2/\epsilon_0 m_{eff})$ depends on the electron density n and on the electron effective mass m_{eff} or optical mass which includes the coupling of the free electrons to the ion core. e is the electron charge and ϵ_0 the vacuum permittivity. γ is the phenomenological damping constant of the bulk material. In the case of a perfectly free electron gas and in the limit of $\gamma \ll \omega$ the width Γ of the plasmon band is given by the damping constant γ.

Combining the resonance condition for eq 1 with the expression for the dielectric constant of a free electron gas (eq 2) one finds that the absorption maximum of the plasmon oscillation is roughly given by

$$\omega_{max} = \frac{ne^2}{\epsilon_0 m_{eff}\sqrt{1+\epsilon_m}} \qquad (3)$$

The electron densities and effective masses of gold and silver and therefore their plasma frequencies are, however, very similar,[41,42,46] and the observed linear shift of the plasmon absorption cannot be explained in this way. In fact, using eq 3 a surface plasmon absorption at 299 and 287 nm is calculated for gold and silver, respectively. This shows that the noble metals gold and silver cannot be treated as simple free electron metals and that eq 3 fails to describe the plasmon absorption which can be considered a hybrid resonance in these metals resulting from cooperative behavior of both the d-band and conduction electrons.[8] The difference in the interband contribution to the plasmon resonance or equivalently the difference in the core polarizability leads to a surface plasmon absorption at 400 nm for silver and even 520 nm for gold nanoparticles.

Therefore, the material dielectric function which includes those core polarization effects and the full Mie expression (eq 1) have to be used to describe the surface plasmon absorption correctly for gold and silver. Assuming now that the dielectric function of the alloy particles takes the form $\epsilon(\alpha) = (1-\alpha)\epsilon_{Au} + \alpha\,\epsilon_{Ag}$,[15,28] the absorption spectra for several compositions are calculated using the Mie equation in the dipole approximation (eq 1). This is illustrated in Figure 4a. The measured real and imaginary parts of the dielectric constants of gold and silver are taken from ref 47. These simulations are also not able to reproduce the experimental results for the alloy particles. Especially a linear dependence of the absorption maximum on the particle composition is not found. But also the shape of the plasmon resonance for the alloy nanoparticles with a gold mole fraction of 0.25 and 0.5 is in poor agreement with experimental results.

This discrepancy can be improved if the dielectric data of Ripken[48] for thin alloy films is used instead. Figure 4b shows the results of that calculation for a gold mole fraction of 0.28. The experimental curve for $x_{Au} = 0.27$ is also included in Figure 4b as the dashed line. Excellent agreement between experiment and theory is found. In conclusion, a linear combination of the complex dielectric constants of gold and silver, as suggested before,[15,28] is therefore not justified when describing the optical properties of mixed nanoparticles. This also leads to the
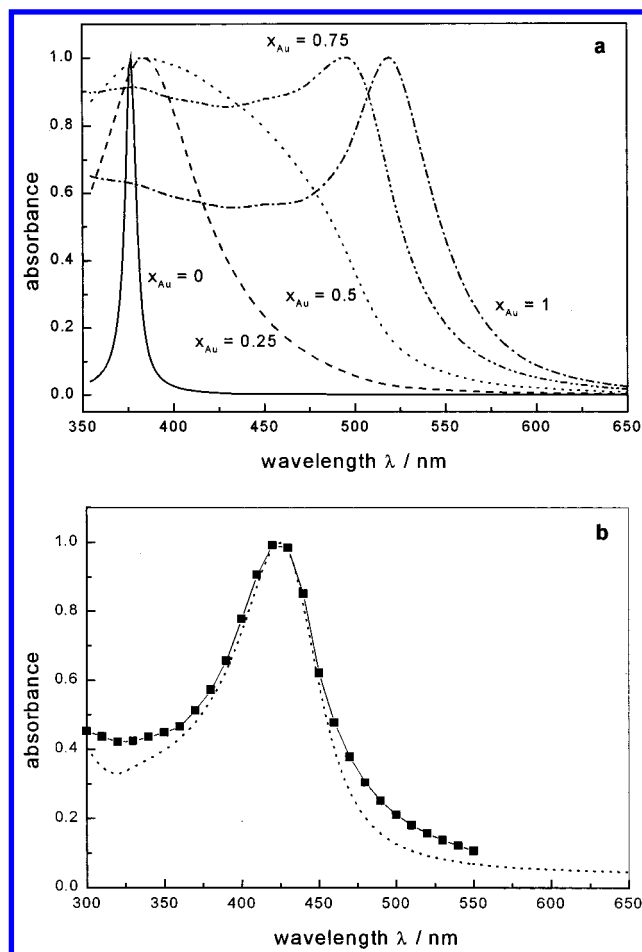

Figure 4. Calculated absorption spectra of gold, silver, and gold–silver alloy nanoparticles using eq 1 (Mie theory in the dipole approximation). For the calculation of the mixed particles a linear combination of the dielectric constant of gold and silver according to the respective gold mol fraction x_{Au} is assumed (a). Part b shows a calculated absorption spectrum using the dielectric data obtained from an alloy film with a gold composition of 0.28% and the corresponding experimental spectrum (dashed line, $x_{Au} = 0.27$).

conclusion that the band structure of the gold–silver alloys is quite different from pure gold or silver. Furthermore, this is an excellent example for demonstrating how important it can be to use the correct form of the material dielectric constant in order to reproduce the shape of the plasmon absorption of metallic nanoparticles.[8]

Conclusion

It is shown how mixed gold–silver nanoparticles with different compositions can easily be obtained in aqueous solution by co-reduction of gold and silver ions with sodium citrate. The formation of alloy particles is confirmed by optical absorption spectroscopy and HRTEM. HRTEM also shows the presence of defect structures such as multiple twins and stacking faults within the alloy particles. Individual islands of gold and silver within the nanoparticles can therefore be ruled out. The maximum of the plasmon absorption is found to vary linearly with the gold mole fraction in agreement with previous work.[25] This can neither be explained by the simple free electron model for the plasmon absorption nor by assuming a linear combination of the dielectric functions of gold and silver. Agreement between experimental data and calculations is found if one uses dielectric data measured on alloy films. This strongly indicates that the plasmon absorption depends critically on the correct material

Letters

J. Phys. Chem. B, Vol. 103, No. 18, 1999 **3533**

dielectric function and its slope. On the other hand, the fact, that a linear dependence is found experimentally, provides a very convenient way of tuning the optical absorption properties of noble metal nanoparticles.

References and Notes

(1) Henglein, A. *J. Phys. Chem.* **1993**, *97*, 8457.

(2) Henglein, A. *Chem. Rev.* **1989**, *89*, 1861.

(3) Alivisatos, A. P. *J. Phys. Chem.* **1996**, *100*, 13226.

(4) Schmid, G. *Clusters & Colloids: From Theory to Application*; VCH: Weinheim 1994.

(5) Kamat, P. V.; Meisel, D. Studies in Surface Science and Catalysis, Vol. 103; *Semiconductor Nanoclusters − Physical, Chemical, and Catalytic Aspects*; Elsevier: Amsterdam, 1997.

(6) Edelstein, A. S.; Cammarata, R. C. *Nanoparticles: Synthesis, Properties and Applications*; Institute of Physics Publishing: Bristol, 1996.

(7) Graetzel, M. In *Electrochemistry in Colloids and Dispersions*; Mackay, R. A., Texter, J., Eds.; VCH: Weinheim, 1992.

(8) Kreibig, U.; Vollmer, M. *Optical Properties of Metal Clusters*; Springer: Berlin, 1995.

(9) Papavassiliou, G. C. *Prog. Solid State Chem.* **1980**, *12*, 185.

(10) Perenboom, J. A. A. J.; Wyder, P.; Meier, P. *Phys. Rep.* **1981**, *78*, 173.

(11) Hughes, A. E.; Jain, S. C. *Adv. Phys.* **1979**, *28*, 717.

(12) Kerker, M. *The Scattering of Light and Other Electromagnetic Radiation*; Academic Press: New York, 1969.

(13) Bohren, C. F.; Huffman, D. R. *Absorption and Scattering of Light by Small Particles*; Wiley: New York, 1983.

(14) Creighton, J. A.; Eadon, D. G. *J. Chem. Soc., Faraday Trans.* **1991**, *87*, 3881.

(15) Mulvaney, P. *Langmuir* **1996**, *12*, 788.

(16) Mie, G. *Ann. Phys.* **1908**, *25*, 377.

(17) Kreibig, U.; Genzel, U. *Surf. Sci.* **1985**, *156*, 678.

(18) Schwank, J. *Gold Bull.* **1983**, *16*, 98.

(19) Schwank, J. *Gold Bull.* **1983**, *16*, 103.

(20) Turkevich, J. *Gold Bull.* **1985**, *18*, 86.

(21) Turkevich, J. *Gold Bull.* **1985**, *18*, 125.

(22) Harada, M.; Asakura, K.; Ueki, Y.; Toshima, N. *J. Phys. Chem.* **1992**, *96*, 9730.

(23) Toshima, N.; Harada, M.; Yamazaki, Y.; Asakura, K. *J. Phys. Chem.* **1992**, *96*, 9927.

(24) Liu, H.; Mao, G.; Meng, S. *J. Mol. Catal.* **1992**, *74*, 275.

(25) Papavassiliou, G. C. *J. Phys. F: Metal Phys.* **1976**, *6*, L103.

(26) Sinzig, J.; Radtke, U.; Quinten, M.; Kreibig, U. *Z. Phys. D* **1993**, *26*, 242.

(27) Liz-Marzan, L. M.; Philipse, A. P. *J. Phys. Chem.* **1995**, *99*, 15120.

(28) Teo, B. K.; Keating, K.; Kao, Y.-H. *J. Am. Chem. Soc.* **1987**, *109*, 3494.

(29) Mulvaney, P.; Giersig, M.; Henglein, A. *J. Phys. Chem.* **1993**, *97*, 7061.

(30) Sato, T.; Kuroda, S.; Takami, A.; Yonezawa, Y.; Hada, H. *Appl. Organomet. Chem.* **1991**, *5*, 261.

(31) Turkevich, J.; Stevenson, P. C.; Hillier, J. *Discuss. Faraday Soc.* **1951**, *11*, 55.

(32) Torigoe, K.; Nakajima, Y.; Esumi, K. *J. Phys. Chem.* **1993**, *97*, 8304.

(33) Mulvaney, P.; Giersig, M.; Henglein, A. *J. Phys. Chem.* **1992**, *96*, 10419.

(34) Carey Lea, M. *Am. J. Sci.* **1889**, *37*, 476.

(35) Turro, N. J. *Modern Molecular Photochemistry*; University Science Books: Mill Valley, 1991.

(36) Wang, Z. L. *Adv. Mater.* **1998**, *10*, 13.

(37) Link, S.; Burda, C.; Wang, Z. L.; El-Sayed, M. A. *J. Chem. Phys.*, submitted.

(38) Buffat, P.-A.; Flueeli, M.; Spycher, R.; Stadelmann, P.; Borel, J.-P. *Faraday Discuss.* **1991**, *92*, 173.

(39) Smith, D. J.; Marks, L. D. *J. Cryst. Growth* **1981**, *54*, 425.

(40) Smith, D. J.; Marks, L. D. *J. Cryst. Growth* **1981**, *54*, 433.

(41) Ashcroft, N. W.; Mermin, N. D. *Solid State Physics*; Saunders College: Philadelphia, 1976.

(42) Kittel, C. *Introduction to Solid State Physics*; Wiley: New York, 1996.

(43) Okamoto, H.; Massalski, T. B. *Phase Diagrams of Binary Gold Alloys*; ASM International: Metals Park, 1987.

(44) Alvarez, M. M.; Khoury, J. T.; Schaaff, T. G.; Shafigullin, M. N.; Vezmer, I.; Whetten, R. L. *J. Phys. Chem. B* **1997**, *101*, 3706.

(45) Kreibig, U.; v. Fragstein, C. *Z. Phys.* **1969**, *224*, 307.

(46) Hummel, R. E. *Optische Eigenschaften von Metallen und Legierungen*; Springer: Berlin, 1971.

(47) Johnson, P. B.; Christy, R. W. *Phys. Rev. B* **1972**, *6*, 4370.

(48) Ripken, K. *Z. Phys.* **1972**, *250*, 228.